Purdue University

Purdue e-Pubs

International Refrigeration and Air Conditioning Conference

School of Mechanical Engineering

2022

The Role of Internal Heat Exchanger in an R744 Vapor Compression System in the Air-conditioning Mode Under Various Conditions

Wenying Zhang

Vladimir Cernicin

Pega Hrnjak

Follow this and additional works at: https://docs.lib.purdue.edu/iracc

Zhang, Wenying; Cernicin, Vladimir; and Hrnjak, Pega, "The Role of Internal Heat Exchanger in an R744 Vapor Compression System in the Air-conditioning Mode Under Various Conditions" (2022). *International Refrigeration and Air Conditioning Conference.* Paper 2303.
https://docs.lib.purdue.edu/iracc/2303

This document has been made available through Purdue e-Pubs, a service of the Purdue University Libraries. Please contact epubs@purdue.edu for additional information.
Complete proceedings may be acquired in print and on CD-ROM directly from the Ray W. Herrick Laboratories at https://engineering.purdue.edu/Herrick/Events/orderlit.html

The Role of Internal Heat Exchanger in an R744 Vapor Compression System in the Air-conditioning Mode Under Various Conditions

Wenying ZHANG [1], Vladimir Cernicin [2], Pega HRNJAK[1, 3]*

[1]ACRC, University of Illinois, Urbana, Illinois, USA
wenying3@illinois.edu

[2]Faculty of Mechanical Engineering, University of Belgrade, Belgrade, Serbia
vcernicin@mas.bg.ac.rs

[3]Creative Thermal Solutions, Inc., Urbana, Illinois, USA
pega@illinois.edu

* Corresponding Author

ABSTRACT

This paper first presents a comprehensive review of the internal heat exchanger, followed by the discussion of experimental results of the role of an internal heat exchanger in an R744 air conditioning system. The effects of refrigerant charge amount on the performance of both basic and internal heat exchanger systems were investigated. Also, the control equations of COP-maximizing high-side pressure were developed and used for both systems. The experimental data show up to 13.8% improvement in efficiency by introducing the internal heat exchanger. The different roles of IHX in sub- and transcritical modes and the reason for the difference are discussed in the paper.

1. INTRODUCTION

Internal heat exchangers (IHXs), also known as suction/liquid line heat exchangers, are widely applied in vapor refrigeration systems to improve efficiency. The essence is to subcool the liquid refrigerant leaving the condenser using the low-pressure low-temperature refrigerant that exits the evaporator. The benefits are increasing the specific cooling capacity of the refrigerant and preventing the liquid refrigerant from entering the compressor. However, the discharge temperature increases as the superheat at the suction point of the compressor increases, and the compressor efficiency might drop if the lubricant performance degrades due to high temperature. Overall, the potential improvement of COP due to the installation of IHX depends on the tradeoff between the increase of specific cooling capacity and the increase of specific compressor work.

The typical first assessment of whether the Coefficient of Performance (COP) increases or not is done based on the cycle analysis for the working fluid and operating conditions. The major factors are the thermodynamic and transport properties of the fluid. Domanski et al. (1994) theoretically evaluated the performance effects of installing IHXs for 29 different refrigerants. The results show the benefits of IHX depend on a combination of operating conditions and fluid properties with specific heat capacity being the most influential property. In addition, the authors developed the method and provided four charts of different refrigerants for evaluation, but a simplified equation or correlation is desired for general applications. Therefore, many researchers continue to explore a simple and general criterion for evaluating the potential benefits of installing IHX using only refrigerant thermodynamic properties and operating temperatures. Aprea et al. (1999) presented a simplified criterion and two application charts for R502 and R32 based on the thermodynamic analysis. The results show that IHX is only advantageous for R502. Klein et al. (2000) proposed a new dimensionless group to correlate performance impacts related to IHX for 11 refrigerants considering the effects of pressure drops through the IHX. It is concluded that IHXs are most useful at high temperature lifts $L = T_{cond} - T_{evap}$ and for refrigerants having a relatively small value of $D = dh_{vap}/(c_{p,l}T_c)$, and the benefits of IHX are reduced due to the pressure drop in it. Mastrullo et al. (2007) developed a graphical method to predict the behavior of installing IHX, changing the operating conditions, refrigerants, and IHX size. The authors concluded that refrigerants with a low COP and high value of $c_{p,v}$ are more positively influenced by introducing

IHX. Hermes (2013) presented a different thermodynamic evaluation of IHX by assuming the same cooling capacity for both basic and IHX cycles, while all previous studies assume the same evaporating pressure for both cycles. The author concluded that there exists an evaporating pressure that maximizes the compressor work for a fixed condensing temperature, cooling capacity, and compressor swept volume rate.

The more detailed analysis considers the size of the heat exchangers, operating conditions, and compressor efficiencies. For various reasons, an indoor evaporator has one-third the size of an outdoor condenser/ gas cooler for typical residential and automobile systems. Also, the airflow rate through the outdoor coil is higher due to less concern for noise, and this increases the effectiveness of the outdoor coil. All the aforementioned reasons lead to the difference between the operation of the vapor compression system in Air-Conditioning (AC) and Heat Pump (HP) mode, as well as the different roles of Internal Heat Exchanger (IHX) in the two modes.

On the other hand, the design of the system varies for different applications, so experimental studies have been conducted for more accurate quantitative studies. For domestic refrigerators and freezers, the simple expansion device- capillary tubes are soldered on the external surfaces of suction lines and work as counterflow IHXs. Staebler (1981) presented capacity balance to calculate the length of diabatic capillary tube for R12 and R22. Bittle (1994) evaluated the capillary IHX performance with R134a and R152a experimentally, considering up to ten different design variables. The author also developed performance prediction equations for both refrigerants, which can be used as design tools for engineers. Melo et al. (2002) conducted comprehensive experiments with R600a for a range of geometries of capillary IHX and operating conditions typical of domestic refrigerators and freezers. Empirical correlations were developed to estimate the refrigerant mass flow rate through the capillary tube and the suction temperature of the compressor. Khan et al. (2009) conducted experiments to study the flow through diabatic spiral capillary tubes, considering the geometric and the arrangement of the capillary IHX. It was concluded that the refrigerant mass flow rate is affected by the suction-line inlet superheat and heat exchange length, in addition to the capillary tube diameter, capillary tube length, coil pitch, and capillary inlet subcooling.

For automobile AC systems, the liquid line is designed as a helix tube and immersed inside the liquid refrigerant in the accumulator for compactness. . In this case, the accumulator heat exchanger (AHX), or known as integrated accumulator and IHX (Acc/IHX), has been investigated by many researchers and engineers. Mei et al. (1994) developed an R134a liquid over-feeding (LOF) mobile air conditioning system that applied an accumulator-heat exchanger. The results indicated an increase of 20% in system cooling capacity and COP at a compressor speed of 2020 RPM. Meyer and Wood (2001) were the first authors to describe a mathematical model of an AHX publicly. They validated the model with an R22 air-conditioning system, and the model predicts the performance of the system within -16% to 13%. Kang et al. (2007) studied the effects of an AHX on the performance of an R22 refrigeration system experimentally. At the same EXV opening of 50%, the cooling capacity and COP of the AHX system were higher than the basic system by 7.5% and 3.2%, respectively.

For transcritical R744 systems, the different design philosophies and control strategies should be applied due to the different properties. Lorentzen and Pettersen (1993) presented a transcritical CO_2 automobile AC system with an accumulator and an IHX, and the data showed that the improvement in COP by internal heat exchanging is mainly due to the reduction of the throttling loss when subcooled liquid CO_2 enters the expansion device. However, this is at a cost of the increased average temperature of heat rejection and irreversibility in the gas cooler. Boewe et al. (1999) conducted experiments with a transcritical CO_2 automobile AC system with an accumulator to study the role of IHX in air-conditioning mode. The results showed that both the capacity and COP were increased by up to 25%, and the benefits of IHX are more significant in high ambient temperature conditions. The IHX reduces the capacity- and efficiency-maximizing discharge pressure and brings them together. This helps to increase the cooling capacity when optimizing the efficiency of the AC system. Kim et al. (2005) investigated the performance of a transcritical CO_2 water heater system with a coaxial IHX numerically and validated experimentally. Also, the efficiency of the system is slightly improved by introducing an IHX up to specific discharge pressure, above which the trend is reversed. Zhang et al. (2011) presented a thermodynamic cycle analysis and an experimental validation to study the effects of an IHX on transcritical CO_2 cycles. The results showed that the COP is slightly reduced by an IHX in the subcritical mode. In the transcritical mode, a transition gas cooler exit temperature exists for a compressor discharge temperature, above which the IHX improves the cycle performance.

Although the effects of IHX on the performance of a transcritical CO_2 refrigeration system have been studied by many researchers, the role of an IHX in a reversible CO_2 AC/HP pump system has not been discussed in public

literature. In this paper (No. 151) and an accompanying paper (No. 153), we will discuss the role of IHX in both AC and HP modes with an experimental illustration of an R744 system under various conditions. The influence of refrigerant charge amount, efficiency-maximizing control equation, and normalized heating performance will be presented. The conclusion can be used to guide the design of reversible R744 air-conditioning systems for different applications.

2. EXPERIMENTAL SETUP

2.1 Facility

The role of IHX in an R744 air-source AC/HP system was investigated experimentally in this paper. A facility with two climate chambers was calibrated and used for this purpose. To control the temperature, humidity, and airflow rate, a glycol heat exchanger, a PID-controlled electric heater, a steam spray, and a wind tunnel with VFD-controlled blowers were installed inside each climate chamber. Figure 1 presents the refrigerant-side sensors and the arrangement of the reversible R744 air-conditioning system inside and between the climate chambers. By controlling the ball valves 1 to 4 (black: closed; white: opened) in the system, the R744 system can be reversed from HP mode to AC mode. Using the ball valves 5 and 6, the high-pressure side of the IHX can be bypassed. The one-slab two-pass outdoor coil (gas cooler in AC mode) and the Electronic Expansion Valve (EXV) for HP mode were installed inside the outdoor climate chamber. The two-slab four-pass indoor coil and the EXV for AC mode were installed inside the indoor climate chamber. The mid-section circuit consists of a semi-hermetic reciprocating compressor, the integrated IHX and accumulator, and the EXV controllers. The dimensions of the key components are listed in Table 1.

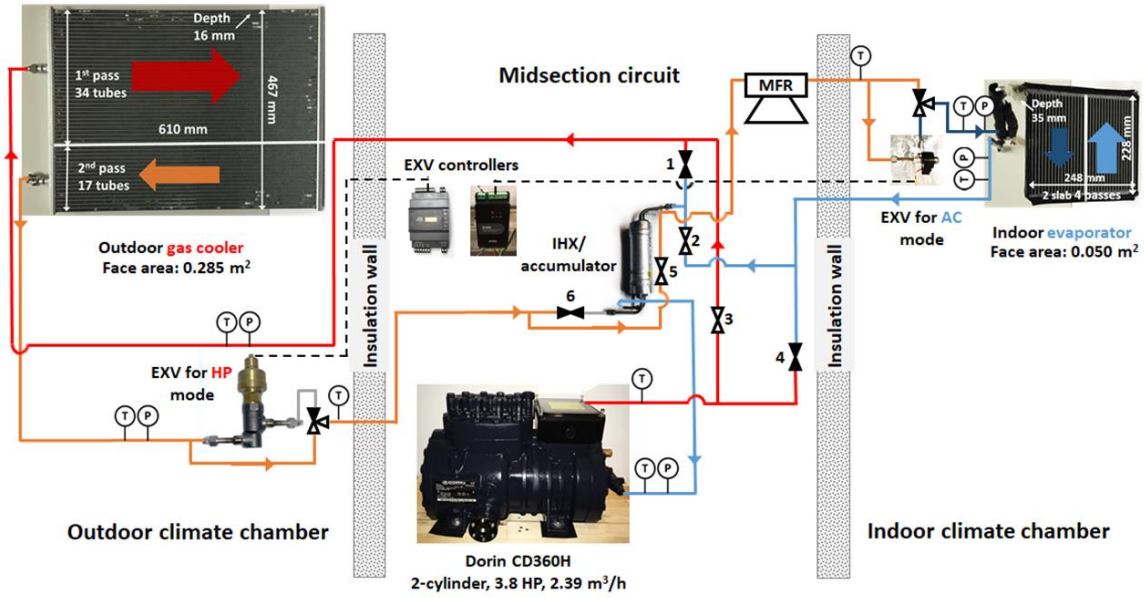

Figure 1: Schematic drawing of the R744 system in AC mode

To measure the steady-state performance of the reversible R744 air-conditioning system, three independent approaches were used: refrigerant-, air-, and chamber-side balances. As shown in Figure 1, pressure transducers, thermocouple probes, and a mass flow meter were installed in the refrigerant circuit. Also, thermocouple grids, dew point sensors, air nozzles, and differential pressure transducers were installed long the wind tunnels. In addition, power transducers were installed to measure the energy consumed inside the climate chamber, and the cooling capacity of the glycol heat exchangers was calculated using measured glycol mass flow rates and inlet/ exit glycol temperatures for both chambers. Considering the heat loss through the insulation walls, the cooling/ heating capacity of indoor/ outdoor coils was calculated using the chamber-side energy balance. Table 2 presents the details and uncertainties of the sensors used in this project. All sensors were calibrated prior installed in the facility. The signals from the sensors are measured by an HP series 75000B data logger and converted to SI-unit parameters via the VEE

program. For each condition, we waited for at least 30 minutes to stabilize the reading and then recorded the data for another 20 minutes with an interval of 6 seconds.

Table 1: Dimensions of key components of the R744 system

Component	Dimensions
Outdoor coil (1-slab, 2-pass: 17/ 34 tubes)	• Overall dimension (mm): 635 (H) × 467 (W) × 16 (T) • Fin height (mm): 8.0 • Fin pitch (mm): 1.3 • Fin thickness (mm): 0.1 • Louver length (mm): 7.2 • Louver pitch (mm): 0.9
Indoor coil (2-slab, 4- pass: all 17 tubes)	• Overall dimension (mm): 229 (H) × 248 (W) × 35 (T) • Fin height (mm): 5.6 • Fin pitch (mm): 1.4 • Fin thickness (mm): 0.08 • Louver length (mm): 4.9 • Louver pitch (mm): 1.12
Internal heat exchanger/ Accumulator	• Overall dimension (mm): 247 (H) × 85 (D) • Counter-flow IHX for AC/ defrost mode • Parallel-flow IHX for HP mode • Nylon accumulator
Semi-hermetic reciprocating compressor	• 2-cylinder • Displacement: 2.39 m^3/h (50 Hz), 2.87 m^3/h (60 Hz) • 1450 rpm @ 50 Hz, 1750 rpm @ 60 Hz • 3.8 HP, 208~ 230V/ 3/ 60 Hz
Electronic expansion valve	• Actuator step range: 2500

Table 2: Uncertainties of refrigerant-, air-, and chamber-side instruments

Parameter	Sensor	Range	Uncertainty
Refrigerant/ glycol temperature [°C]	T-type thermocouple	-50 to 150	± 0.2
Refrigerant low-side pressure [MPa]	Strain gage	0 to 6.89	± 0.003
Refrigerant high-side pressure [MPa]	Strain gage	0 to 20.68	± 0.007
Refrigerant/ glycol mass flow rate [kg/h]	Coriolis-type	0 to 2180/ 0 to 6800	± 0.10% of reading
Electrical power consumption [kW]	3-phase wattmeter	0 to 6	± 0.20% of reading
Air/ wall temperature [°C]	T-type welded thermocouple	-50 to 150	± 0.2
Dew point temperature [°C]	Chilled mirror dew point sensor	-80 to 85	± 0.2
Pressure drop of air-side [Pa]	Differential pressure transducer	0 to 600	± 0.25% of full scale

2.2 Data reduction and uncertainty analysis

The cooling/ heating capacities of indoor/ outdoor coil in the R744 system with and without IHX were calculated using refrigerant-, air-, and chamber-side balances. The thermodynamic properties were calculated using commercial software- Refprop 9.0 (Lemmon. et al., 2010). For the indoor evaporator, the three balances are shown below:

$$Q_{cooling,ref} = (1-OCR)\dot{m}_r(h_{ero} - h_{eri}) + OCR \cdot \dot{m}_r(h_{eoo} - h_{eoi}) \quad \textbf{Eqn (1)}$$

$$Q_{cooling,air} = \dot{m}_{eai,dry}(h_{eai} - h_{eao}) \quad \textbf{Eqn (2)}$$

$$Q_{cooling,cham} = \sum P_{id,elec} - Q_{id,loss} - \dot{m}_{id,g}(T_{id,go} - T_{id,gi}) \quad \textbf{Eqn (3)}$$

Where OCR is the Oil Circulation Rate and was measured by the sampler installed across the mass flow meter on the liquid line. In this project, the OCR is measured to be 2% and the effects on system capacity are negligible. $\dot{m}_r$ was measured by the mass flow meter, and it is actually the mass flow rate of the oil and CO_2 mixture. Refrigerant enthalpy h_{eri} equals the refrigerant enthalpy at EXV inlet h_{xri}, assuming isenthalpic expansion. Refrigerant enthalpy h_{ero}, oil enthalpies h_{eoi} and h_{eoo} were determined from the pressures and temperatures measured at the inlet (T_{eri} and P_{eri}) and outlet (T_{ero} and P_{ero}) of the indoor coil. The refrigerant-side calculation for the evaporator is only valid when there is at least 3°C of superheat at the evaporator exit. Otherwise, the cooling capacity and related refrigerant properties are calculated using the other two approaches.

The indoor air mass flow rate $m_{eai,dry}$ was calculated using measured air temperature (T_{ean}), dew point (T_{dpen}), and pressure drop (DP_{en}) at the indoor nozzles. The enthalpies of air h_{eai} and h_{eao} were determined using air temperatures at the indoor coil inlet T_{eai} and exit T_{eao}. In the calculation, dry air properties were used because dew point measurements showed there was no water condensation across the indoor coil.

The electrical power consumption $P_{id,elec}$ of each device inside the indoor chamber was measured using power transducers. The heat loss from the indoor climate chamber to the ambient $Q_{id,loss}$ was calculated using the measured UA value of the climate chamber. The mass flow rate of glycol flowing into the indoor chamber $m_{id,g}$ and the inlet and exit glycol temperatures ($T_{id,gi}$ and $T_{id,go}$) were used to calculate the cooling capacity of the glycol heat exchanger.

Similarly, three approaches were used to calculate the heating capacity of the outdoor gas cooler：

$$Q_{heating,ref} = (1-OCR)\dot{m}_r(h_{cri} - h_{cro}) + OCR \cdot \dot{m}_r(h_{coi} - h_{coo}) \quad \textbf{Eqn (4)}$$

$$Q_{heating,air} = \dot{m}_{cai,dry}(h_{cao} - h_{cai}) \quad \textbf{Eqn (5)}$$

$$Q_{heating,cham} = \dot{m}_{od,g}(T_{od,go} - T_{od,gi}) + Q_{od,loss} - \sum P_{od,elec} \quad \textbf{Eqn (6)}$$

Also, for the IHX cycle, the capacity of the IHX was calculated using the high-pressure refrigerant-side, since it is in the supercritical or subcooled zone:

$$Q_{IHX,ref} = (1-OCR)\dot{m}_r(h_{cro} - h_{xri}) + OCR \cdot \dot{m}_r(h_{coo} - h_{xoi}) \quad \textbf{Eqn (7)}$$

Where, refrigerant enthalpy h_{xri} and oil enthalpy h_{xoi} were determined from the pressure and temperature measured at the inlet of the expansion valve. The low-pressure side capacity of IHX equals the high-pressure side capacity, assuming no heat loss to the ambient.

The Coefficient of Performance (COP) of the R744 air-conditioning system with and without IHX was calculated as follows:

$$COP = \frac{Q_{cooling,ave}}{P_{comp}} \quad \textbf{Eqn (8)}$$

Where, $Q_{cooling,ave}$ is the average of ref-, air-, and chamber-side cooling capacity of indoor evaporator. P_{comp} is the measured electrical power consumption of the VFD-controlled compressor.

The uncertainty analysis was conducted using a MATLAB program integrated with the data reduction program, following the method of Moffat (1988). According to the method, the uncertainty in a calculated value R, which is a function of N independent measurements (X_1, X_2, X_3, ... X_N), can be calculated as Eqn (9):

$$\delta R = \left(\sum_{i=1}^{N} \left(\frac{\partial R}{\partial X_i} \delta X_i \right)^2 \right)^{\frac{1}{2}} \quad \textbf{Eqn (9)}$$

Where uncertainty of each measurement is determined using Eqn (10):

$$\delta X_i = \left(\delta X_{i,A}{}^2 + \delta X_{i,B}{}^2 \right)^{\frac{1}{2}} \quad \textbf{Eqn (10)}$$

Where, $\delta X_{i,A}$ is the type-A uncertainty of measurement X_i, which was calculated as the standard deviation of each group of data recorded every 20 minutes. The type-B uncertainty $\delta X_{i,B}$ was either provided by the manufacturer or by the calibration: it is ±0.2℃ for the refrigerant temperatures after we calibrated the type-T thermocouples with RTD sensors (PT100).

For the indoor cooling capacity, the uncertainties were 2.2%, 6.2%, and 0.5% for ref-, air-, and chamber-side approaches. Overall, the most reliable approach is the chamber-side due to the simplicity of energy conservation, while the airside is the least accurate one because of the high volumetric flow rate of indoor air.

3. RESULTS AND DISCUSSION

In this paper, the role of IHX in an R744 vapor compression system operating both in subcritical and transcritical modes was studied experimentally. To compare the performance of the system with and without the IHX, we first tuned both basic and IHX systems to have the optimal refrigerant charge amounts and the efficiency-maximizing controls. Then, the performance of the basic and the IHX systems were compared and analyzed. Table 3 lists all the experimental conditions in this paper. The details and the results will be discussed in the following chapter.

Table 3: Operating conditions of all experiments in this paper

	The purpose of this group	T_{eai} **[℃]**	RH_{eai} **[%]**	V_{eai} **[m/s]**	T_{cai} **[℃]**	V_{cai} **[m/s]**	**Compressor speed [%]**
Group 1	Optimal charge amounts	40	20	2.5	40	3.0	70
Group 2	Control equations	25 to 40			25 to 40		60 to 75
Group 3	Steady-state experiments	25 to 40			25 to 40		60 to 90

3.1 Effects of refrigerant charge amount on the system performance- Group 1

The effects of the refrigerant charge amount on the R744 vapor compression system with and without IHX are presented in the section. Figure 2(a) and (b) show the cooling capacity, compressor power consumption, COP, and refrigerant quality at the evaporator exit for the basic system and IHX system as the charge amount increases. Figure 2(c) and (d) present the refrigerant mass flow rate, pressure, and temperature of the refrigerant at different locations of each system during the charging experiments.

The charging experiments were conducted following the procedure in the SAE standard (SAE J2765, 2008). The ambient air temperature T_{cai} and in-cabin air temperature T_{eai} were 40℃. The in-cabin humidity was controlled to eliminate condensation happening on the in-cabin evaporator. The outdoor air velocity was 3.0 m/s, and the in-cabin air flow rate was 2.5 m/s in the charging experiments. The compressor speed was fixed at 70% of the full speed (1450 rpm). During the charging procedure, CO_2 was added to the system in front of the Acc/IHX in increments of 50g, then stabilized for at least 30 minutes before recording data for another 20 minutes. For each charge amount, at least three different high-side pressures were tested to find the COP-maximizing pressure, which is presented in Figure 2(c) and (d) as P_{cro}.

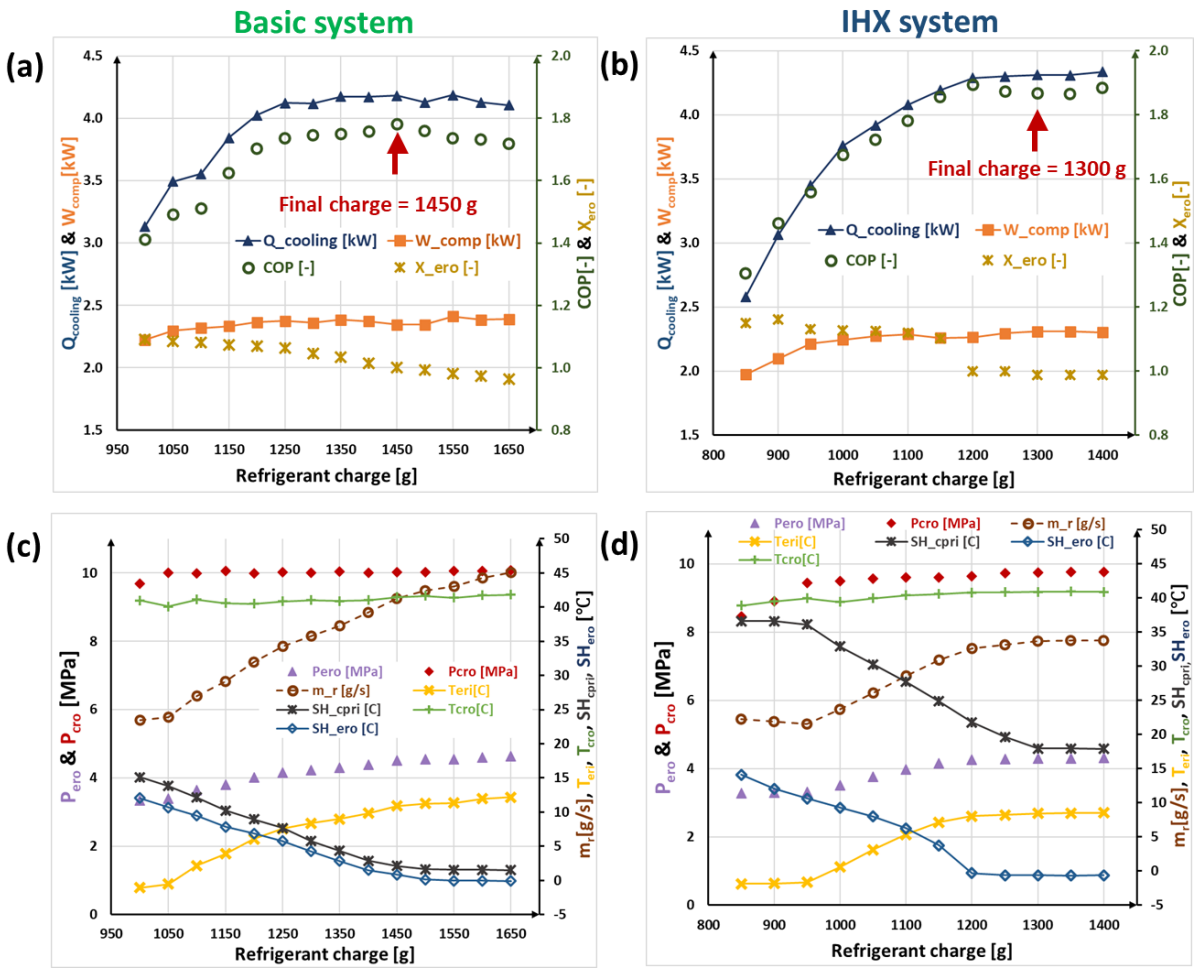

Figure 2: Results of charging experiments for the basic and IHX AC systems

For both basic and IHX systems, the cooling capacity $Q_{cooling}$ and COP increase as the refrigerant charge amount increases and reach a plateau as the charge amount increases to 1350 g for the basic system and 1200 g for the IHX system, as shown in Figure 2(a) and (b). The compressor power consumption W_{comp} has a similar trend but reaches the plateau earlier than cooling capacity and COP. In other words, W_{comp} is sensitive to charge amount when the system is extremely undercharged, but it becomes stable when the refrigerant charge amount is close to the proper charge amount. Also, the evaporator exit quality X_{ero} is decreasing below 1.0 as the charge amount increases to 1500 g for the basic system and 1300 g for the IHX system. The qualities indicate the evaporator is flooded and the heat transfer area is fully used. Also, it shows two-phase refrigerant enters the accumulator, and the system is well charged. Finally, the refrigerant charge amount was optimized to be 1450 g for the basic system to avoid too much liquid refrigerant entering the reciprocating compressor. In the meanwhile, it is chosen to be 1300 g for the IHX system, because liquid refrigerant is stored in the accumulator and the performance becomes stable starting at this point. Comparing the performance of both systems with the final charge, introducing IHX improves the $Q_{cooling}$ and COP by 3.2% and 4.9% at the test condition. This also reduces the charge amount by 150 g, which is 10.3% of the total charge amount of 1450 g.

For both systems, the gas cooler exit temperatures T_{cro} are stabilizing at about 41°C when the systems are well-charged; however, the COP-maximizing pressure P_{cro} is 10.1 MPa for the basic system and 9.7 MPa for the IHX system in the test condition. This agrees with previous studies that the COP-maximizing pressure will be reduced by introducing IHX into a transcritical CO_2 system (Boewe et al., 1999; Cho et al., 2007). The major difference between the two systems during the charging procedure is: the refrigerant mass flow rate m_r increases and reaches a plateau of 33.8 g/s for the IHX system, while it continues increasing as refrigerant is added to the basic system. This is because vapor CO_2 with fixed superheat SH_{cpri} leaves the low-pressure side of IHX and enters the compressor for

the IHX system during the charging procedure, as shown in Figure 2(d). But two-phase refrigerant with decreased quality (x_{cpri}= x_{ero} for the basic system) enters the compressor for the basic system during the charging procedure (Figure 2 (a)), which might cause a failure of the reciprocating compressor. In this case, the volumetric efficiency of the compressor is significantly increased for the basic system, and the refrigerant mass flow rate is proportional to the charge amount, as shown in Figure 2(c).

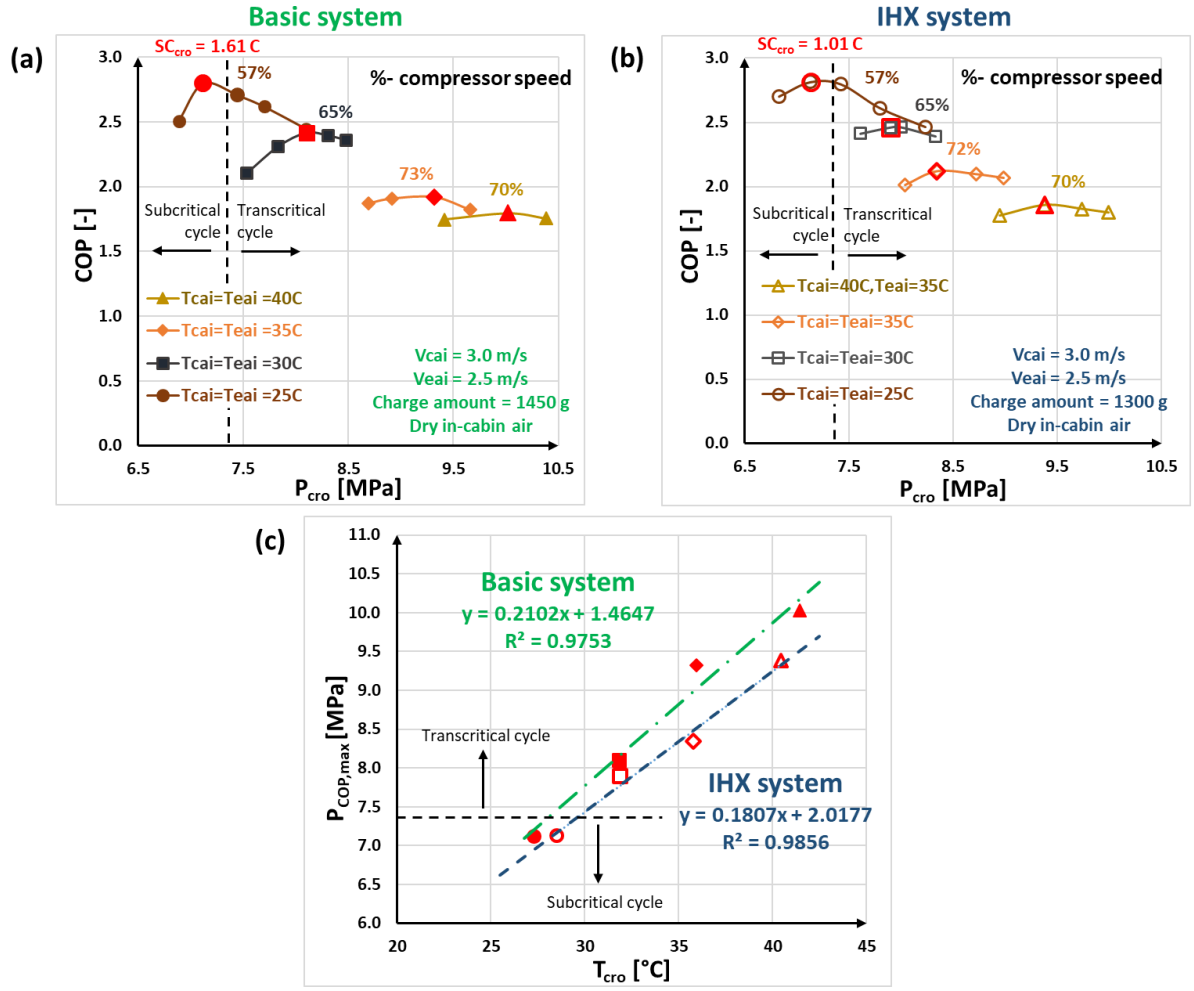

Figure 3: The performance data and high-side pressure control equations for the basic and IHX AC systems

3.2 Effects of IHX on the control equations- Group 2

To achieve the optimal system performance in a wide range of operating temperatures, control equations, instead of a fixed EXV opening, were developed for both basic and IHX systems to maximize efficiency. The high-side pressure control theory was discussed in detail and a graphical method was developed using ideal cycle analysis in the paper of Inokuty (1928). Due to the trade-off between the specific cooling capacity and specific compressor work, there exits one COP-maximizing high-side pressure for a fixed refrigerant gas cooler exit temperature. In practice, the equation is developed using experimental data due to various performances of different gas coolers and compressors, like the approaching temperature and isentropic efficiency.

Figure 3(a) and (b) show the COP curves as functions of the refrigerant pressure at the gas cooler exit P_{cro} for the basic and IHX systems. The control variables including the operating temperatures, airflow rates (AFRs), charge amounts, and compressor speeds are listed in the charts. The maximum COP and related T_{cro} are highlighted in red and then used to develop the control equations for both systems, as presented in Figure 3(c). The results show that both basic and IHX systems reach the maximum efficiency operating in subcritical modes with 1.61 and 1.01°C of subcooling at the gas cooler/ condenser exit when the ambient temperature T_{cai} is 25°C. For higher ambient-temperature conditions, the maximum COPs are obtained in transcritical modes for both systems. Especially, the

simple linear control equations we developed work well for both subcritical and transcritical modes. Also, Figure 3(c) shows that introducing IHX reduces $P_{COP,max}$ by 0.24 to 0.67 MPa, and this reduction is more significant when the ambient temperature is increased.

3.3 Effects of IHX on the AC system performance under various conditions- Group 3

After fine-tuning the basic and IHX systems, we conducted experiments in the steady-state and pull-down scenarios to investigate the role of IHX in an R744 AC system. In the steady-state scenario, the indoor air inlet (T_{eai}) and exit (T_{eao}) temperatures are fixed to be 25 and 5°C, while the ambient air temperature T_{cai} varies from 25 to 40°C. In the pull-down scenario, T_{cai} is 40°C, T_{eai} changes from 25 to 40°C, and the indoor air exit temperature T_{eao} is always 20°C lower than T_{eai}. The compressor speed is adjusted to match the cooling capacity, and all other control parameters are listed in the charts in Figure 4.

Figure 4(a) and (b) show the experimental results of the COP of both basic and IHX systems and the COP improvement by introducing IHX. For low ambient temperature conditions (T_{cai}= T_{eai}= 25°C), both systems operate in subcritical mode and IHX has a negligible effect (only 1.2%) on the system efficiency. While IHX improves the system efficiency from 5.9% to 13.8% when both systems are operating in transcritical mode and at higher ambient temperatures.

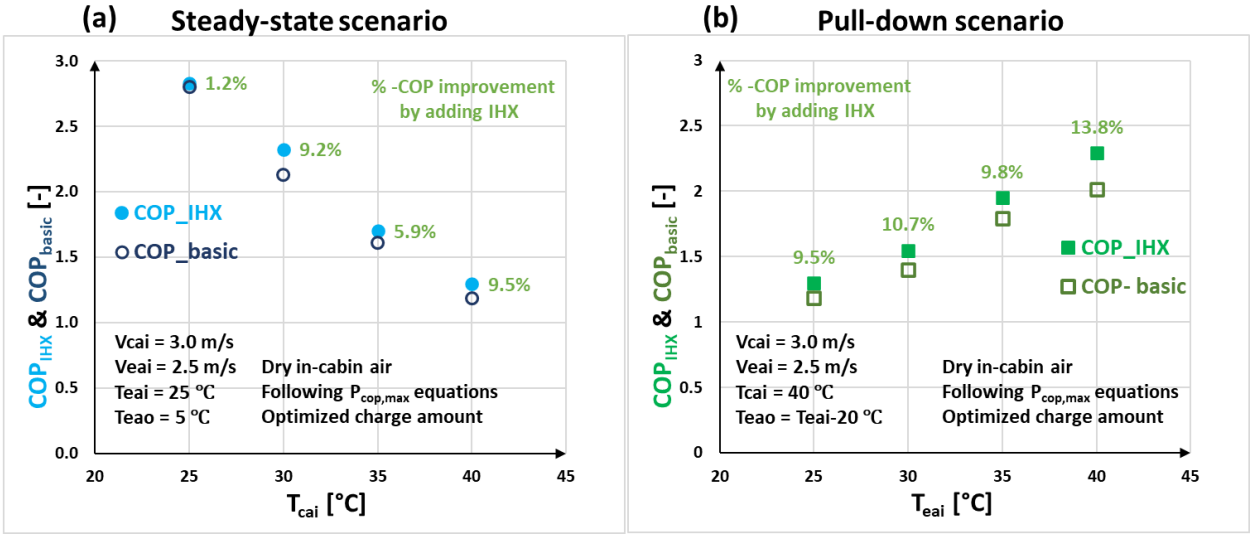

Figure 4: The performance data and benefits of IHX in steady-state and pull-down scenarios

Figure 5(a) and (b) show the experimental results of the P-h plots of both basic and IHX systems in typical subcritical and transcritical operating conditions. For the subcritical condition (T_{cai}= T_{eai}= 25°C), introducing IHX reduces refrigerant quality at evaporator inlet x_{ero} and thus improves the refrigerant distribution in the evaporator. However, IHX has insignificant effects on both evaporating and condensing pressure. In addition, IHX reduces throttling loss negligibly by reducing the temperature at EXV inlet from 27.82 to 19.68°C, because the inlet of EXV is in the subcooled liquid zone for both systems. However, IHX reduces the refrigerant density at the compressor suction point from 100.3 to 78.79 kg/m^3 and the refrigerant flow rate from 26.72 to 23.24 g/s. Overall, IHX has limited benefits for R744 AC systems operating in subcritical mode. On the contrary, for the transcritical condition (T_{cai}= T_{eai}= 40°C), introducing IHX significantly lower the high-side pressure and raises the evaporating pressure by 8% and 7%, respectively. As a result, the compression ratio reduces from 2.21 to 1.89, and the volumetric efficiency and mass flow rate increase, while the compressor power consumption reduces by 15%. Also, the throttling loss is reduced as the compression ratio decreases. In conclusion, IHX improves the system performance significantly in transcritical mode.

4. CONCLUSIONS

An R744 air-conditioning system was built to study the role of IHX in both subcritical and transcritical modes experimentally. The results show:

- The IHX system requires less refrigerant charge amount than the basic system in the most challenging condition- when the ambient temperature is 40℃.
- Introducing IHX reduces $P_{COP,max}$ by 0.24 to 0.67 MPa, and this reduction is more significant when the ambient temperature is increased.
- IHX has a negligible effect on system efficiency when the AC system is operating in subcritical mode, while it improves system efficiency by up to 13.8% when the AC system is operating in transcritical mode and with higher ambient temperature conditions.

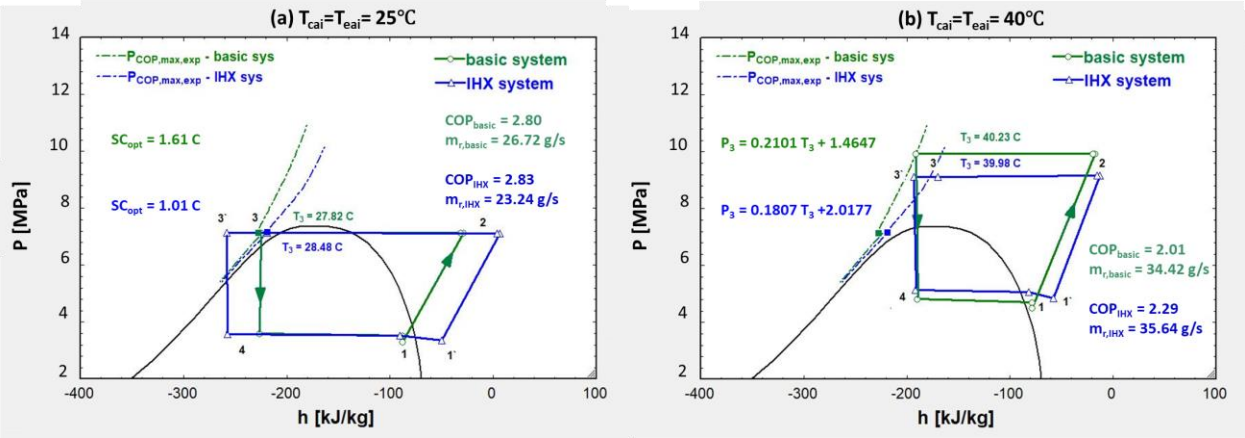

Figure 5: The P-h plots of basic and IHX systems in subcritical and transcritical mode

NOMENCLATURE

AC	air-conditioning	$\dot{m}_r$	mass flow rate [kg/s]
Acc	accumulator	**OCR**	oil circulating ratio [-]
COP	Coefficient of Performance	**P**	pressure [bar]
DP	differential pressure [Pa]	**Q**	capacity [kW]
EXV	electronic expansion valve	**T**	temperature [℃]
h	enthalpy [kJ/kg-℃]	**V**	velocity [m/s]
HP	heat pump	**W**	power [kW]
IHX	internal heat exchanger	**x**	quality [-]
M	mass [kg]		

Subscript

a/ air	air-side	i	inlet
acc	accumulator	id	indoor
c	Condenser/ gas cooler	n	nozzle
cham	Chamber-side	o	outlet
cp/ comp	compressor	od	outdoor
e	evaporator	oi	oil inlet
elec	electricity	oo	oil outlet
high	high-pressure side	r/ ref	refrigerant-side
g	glycol	x	expansion valve

REFERENCES

Aprea, C., Ascani, M., & De Rossi, F. (1999). A criterion for predicting the possible advantage of adopting a suction/liquid heat exchanger in refrigerating system. *Applied Thermal Engineering*, *19*(4), 329–336. https://doi.org/10.1016/s1359-4311(98)00070-2

Bittle, R. R. (1994). *An experimental evaluation of capillary tube- suction line heat exchanger performance with*

alternative refrigerants HFC-134a and HFC-152a. Iowa State University.
Boewe, D., Yin, J., Park, Y. C., Bullard, C. W., & Hrnjak, P. S. (1999). The role of suction line heat exchanger in transcritical R744 Mobile A/C systems. *SAE Technical Papers*, *724*. https://doi.org/10.4271/1999-01-0583
Cho, H., Ryu, C., & Kim, Y. (2007). Cooling performance of a variable speed CO2 cycle with an electronic expansion valve and internal heat exchanger. *International Journal of Refrigeration*, *30*(4), 664–671. https://doi.org/10.1016/j.ijrefrig.2006.10.004
Domanski, P. A., Didion, D. A., & Doyle, J. P. (1994). Evaluation of suction-line/liquid-line heat exchange in the refrigeration cycle. *International Journal of Refrigeration*, *17*(7), 487–493. https://doi.org/10.1016/0140-7007(94)90010-8
Hermes, C. J. L. (2013). Alternative evaluation of liquid-to-suction heat exchange in the refrigeration cycle. *International Journal of Refrigeration*, *36*(8), 2119–2127. https://doi.org/10.1016/j.ijrefrig.2013.06.007
Inokuty, H. (1928). Graphical Method of finding compression pressure of CO2 refrigerating machine for maximum coefficient of performance. *Proceedings of the 5th IIR International Congress of Refrigeration*, 185–192.
Kang, H., Choi, K., Park, C., & Kim, Y. (2007). Effects of accumulator heat exchangers on the performance of a refrigeration system. *International Journal of Refrigeration*, *30*(2), 282–289. https://doi.org/10.1016/j.ijrefrig.2006.07.009
Khan, M. K., Kumar, R., & Sahoo, P. K. (2009). Experimental investigation on diabatic flow of R-134a through spiral capillary tube. *International Journal of Refrigeration*, *32*(2), 261–271. https://doi.org/10.1016/j.ijrefrig.2008.05.010
Kim, S. G., Kim, Y. J., Lee, G., & Kim, M. S. (2005). The performance of a transcritical CO2 cycle with an internal heat exchanger for hot water heating. *International Journal of Refrigeration*, *28*(7), 1064–1072. https://doi.org/10.1016/j.ijrefrig.2005.03.004
Klein, S. A., Reindl, D. T., & Brownell, K. (2000). Refrigeration system performance using liquid-suction heat exchangers. *International Journal of Refrigeration*, *23*(8), 588–596. https://doi.org/10.1016/S0140-7007(00)00008-6
Lemmon, E.W., Huber, M.L., McLinden, M. O. (2010). *NIST Standard Reference Database 23: Reference Fluid Thermodynamic and Transport Properties-REFPROP, Version 9.0*. National Institute of Standards and Technology, Standard Reference Data Program.
Lorentzen, G., & Pettersen, J. (1993). A new , efficient and environmentally benign system for car air-conditioning. *International Journal of Refrigeration*, *16*(1), 4–12.
Mastrullo, R., Mauro, A. W., Tino, S., & Vanoli, G. P. (2007). A chart for predicting the possible advantage of adopting a suction/liquid heat exchanger in refrigerating system. *Applied Thermal Engineering*, *27*(14–15), 2443–2448. https://doi.org/10.1016/j.applthermaleng.2007.03.001
Mei, V. C., Chen, F. C., & Sullivan, R. (1994). *Experimental study of a liquid over-feeding mobile air conditioning system*. 91–94.
Melo, C., Torquato Vieira, L. A., & Pereira, R. H. (2002). Non-adiabatic capillary tube flow with isobutane. *Applied Thermal Engineering*, *22*(14), 1661–1672. https://doi.org/10.1016/S1359-4311(02)00072-8
Meyer, J. P., & Wood, C. W. (2001). The design and experimental verification of heat exchanger accumulators used in small commercially available air conditioning systems. *International Journal of Energy Research*, *25*(10), 911–925. https://doi.org/10.1002/er.728
Moffat, R. J. (1988). Describing the uncertainties in experimental results. *Experimental Thermal and Fluid Science*, *1*(1), 3–17.
SAE, J. (n.d.). *2765. Procedure for measuring system COP (coefficient of performance) of a mobile air conditioning system on a test bench. 2008*.
Staebler, L. (1981). Theory and use of a capillary tube for liquid refrigerant control. *Refrigerating Eng*, *23*(1), 62–64.
Zhang, F. Z., Jiang, P. X., Lin, Y. S., & Zhang, Y. W. (2011). Efficiencies of subcritical and transcritical CO2 inverse cycles with and without an internal heat exchanger. *Applied Thermal Engineering*, *31*(4), 432–438. https://doi.org/10.1016/j.applthermaleng.2010.09.018

ACKNOWLEDGEMENT

This work was supported by all members of ACRC at the University of Illinois at Urbana-Champaign. All the help from our members are gratefully acknowledged!